Peak Non-Gaussian Wind Effects for Database-Assisted Low-Rise Building Design

by

Fahim Sadek and Emil Simiu
Building and Fire Research Laboratory
National Institute of Standards and Technology
Gaithersburg, MD 20899 USA

Reprinted from Journal of Engineering Mechanics, Vol. 128, No. 5, 530-539, May 2002.

NIST
National Institute of Standards and Technology
Technology Administration, U.S. Department of Commerce

Peak Non-Gaussian Wind Effects for Database-Assisted Low-Rise Building Design

Fahim Sadek, M.ASCE,[1] and Emil Simiu, F.ASCE[2]

Abstract: Current procedures for estimating the peaks of the stochastic response of tall buildings to wind are based on the assumption that the response is Gaussian. Those procedures are therefore inapplicable to low-rise buildings, in which time histories of wind-induced internal forces are generally non-Gaussian. In this paper, an automated procedure is developed for obtaining from such time histories sample statistics of internal force peaks for low-rise building design and codification. The procedure is designed for use in software for calculating internal force time series by the database-assisted design approach. A preliminary step in the development of the procedure is the identification of the appropriate marginal probability distribution of the time series using the probability plot correlation coefficient method. The result obtained is that the gamma distribution and a normal distribution are appropriate for estimating the peaks corresponding, respectively, to the longer and shorter tail of the time series' histograms. The distribution of the peaks is then estimated by using the standard translation processes approach. It is found that the peak distribution can be represented by the Extreme Value Type I (Gumbel) distribution. Because estimates obtained from this approach are based on the entire information contained in the time series, they are more stable than estimates based on observed peaks. The procedure can be used to establish minimum acceptable requirements with respect to the duration and sampling rate of the time series of interest, so that the software used for database-assisted design will be both efficient and accurate.

DOI: 10.1061/(ASCE)0733-9399(2002)128:5(530)

CE Database keywords: Buildings, low-rise; Building codes; Probability distribution; Wind loads; Structural reliability; Databases.

Introduction

The risk-consistent, safe, and economical design of low-rise structures subjected to high winds requires realistic estimates of wind effects on components and wind-load resisting systems such as, for example, frames. Inherent in current standard provisions are simplifications due, among other reasons, to the earlier use of the slide rule for calculations of wind loads. The peak effects obtained by using such simplified provisions can differ substantially and erratically from the peak effects induced by the actual, fluctuating wind. Additional simplifications in current standards are due to (a) the use in the development of the codified wind loading of hard-wired ''generic'' influence lines that differ from the actual influence lines of the structure being designed, and (b) the disregard of certain spatial pressure correlation effects, owing to which the codified loads are incorrectly assumed to be independent of the distance between frames.

In recognition of these shortcomings, the ASCE 7-98 Standard (1998) allows the use of records of fluctuating wind pressures obtained in the wind tunnel for each of a sufficiently large number of directions at hundreds of locations on the building envelope. These records are contained in databases and are based on a number of wind tunnel model geometries that, in the long run, can be substantially larger than the relatively modest number of geometries used to develop the current ASCE 7 Standard wind loading provisions. The records can be used to compute time series of internal forces (bending moments, shear forces, and normal forces) in wind-force resisting low-rise building frames using efficient, user-friendly software [e.g., *WiLDE-LRS* (Wind Load Design Environment for Low-Rise Structures); Whalen et al. 2000]. Design that utilizes such databases and software is referred to as database-assisted design (DAD). Inputs to the software are the relevant aerodynamic coefficient databases, the terrain exposure, the extreme wind speed, the geometry of the building, the distance between frames, and the frames' influence lines. The output consists of the time histories of the internal forces for any wind direction at any desired number of cross sections in each of the building's frames.

For design and structural reliability estimation purposes, it is necessary to estimate the largest peak of the internal forces of interest. Current DAD software uses as an estimator of the peak the observed largest peak in an approximately 1 h (prototype) sample record (corresponding to an approximately 1 min wind tunnel record), the sampling rate being 6–8 Hz (prototype), or about 400 Hz for the model (Lin and Surry 1997). This estimator, however, has large variability. As an alternative, information on the largest peaks may be obtained by making use of all the data contained in the time series. This approach has two advantages. First, it yields more stable estimates. Second, it yields useful information on the probability distribution of the peaks. Together with information—based on measurements, statistical estimates, and/or engineering judgment—on wind speeds, terrain roughness, and other relevant parameters, the information on the distribution

[1]Research Associate, Building and Fire Research Laboratory, National Institute of Standards and Technology, Gaithersburg, MD 20899-8611.

[2]NIST Fellow, Building and Fire Research Laboratory, National Institute of Standards and Technology, Gaithersburg, MD 20899-8611.

Note. Associate Editor: George Deodatis. Discussion open until October 1, 2002. Separate discussions must be submitted for individual papers. To extend the closing date by one month, a written request must be filed with the ASCE Managing Editor. The manuscript for this paper was submitted for review and possible publication on June 5, 2001; approved on October 1, 2001. This paper is part of the ***Journal of Engineering Mechanics***, Vol. 128, No. 5, May 1, 2002. ©ASCE, ISSN 0733-9399/2002/5-530–539/$8.00+$.50 per page.

of the peaks is needed to perform structural reliability estimates for wind effects. Such estimates are similar in principle to those developed by Ellingwood et al. (1980). However, owing to vastly increased computer capabilities and to significant wind engineering advances, they can be far more realistic and useful for design, codification, and loss estimation purposes (Minciarelli et al. 2001).

This paper describes the development of an efficient automated procedure for estimating peaks, designed for use with the DAD software. Current procedures for estimating the peaks of the stochastic response of tall buildings to wind are based on the assumption that the response is Gaussian. Those procedures are inapplicable to low-rise buildings, in which time histories of wind-induced internal forces are generally non-Gaussian. The procedure presented in this paper is applicable to non-Gaussian processes and utilizes information contained in a whole sample record, rather than at just one instant in time. The estimation of distributions of non-Gaussian peaks is based on the standard translation processes approach (Grigoriu 1995). This approach requires fitting an optimal marginal distribution to the time series of interest. Subsequent sections show how this task is performed and the results obtained are described. Two variants of the translation processes approach are tested, and the reason for the choice of one of the variants is explained. The input to the procedure consists of the time series of the internal forces, and the output consists of the sample means, standard deviations, and quantiles of the respective peaks. In addition, it is shown how the procedure can be used to ensure that the DAD software is both efficient and accurate.

The next section identifies the appropriate marginal probability distribution of the sample records. This is accomplished using the so-called probability plot correlation coefficient (PPCC) method (Filliben 1975), which identifies the most appropriate distribution from among a set of candidate families of distributions. The third section describes the translation processes-based procedure for the statistical estimation of peaks of non-Gaussian processes. Subsequent sections present examples of the application of the procedure to internal force records, and provide guidance on establishing record lengths and sampling rates that minimize data storage requirements and computation times while ensuring that peaks are estimated accurately.

Selection of Marginal Probability Distributions

A preliminary step in the development of procedures for estimating the largest peaks is to select appropriate marginal probability distributions for the time histories of wind effects. Earlier studies (e.g., Gioffrè et al. 2000) have shown that internal force time histories in low-rise building frames are in general non-Gaussian. Instead of relying on visual inspection, as has been done in many instances in the past, the selection of the most appropriate distribution is accomplished by using the probability plot correlation coefficient (PPCC) method (Filliben 1975; Simiu and Scanlan 1996, p. 614). For any given family of three-parameter distributions (with a shape, location, and scale parameter), a PPCC plot is generated by plotting the correlation coefficient of the probability plot against the shape parameter. The value of the shape parameter that maximizes the correlation coefficient, i.e., has the straightest plot on probability paper, is the optimal shape parameter for that family of distributions. (A PPCC value of 1.0 is the theoretical value corresponding to perfect correlation.) The PPCC plots are obtained in this study by using *Dataplot* software (Dataplot 1996).

In addition to finding an appropriate estimate of the shape parameter for a given family of distributions, the PPCC method is useful for deciding which distributional family is most appropriate. This is done by comparing the PPCC's corresponding to the respective optimal shape parameters in several candidate families of distributions. This criterion implies selecting the distribution that yields the largest PPCC. For example, if the maximum PPCC's for a gamma distribution and for the Extreme Value Type I distribution are, respectively, 0.99 and 0.96, then it can be concluded that the gamma distribution is the more appropriate model.

The candidate distributions considered in this study were the normal distribution, the Extreme Value Type I (Gumbel) distribution, and the gamma distribution. Other distributions such as the beta, exponential, Weibull, and log-normal distributions were initially considered but were eliminated after an assessment of their adequacy. The normal and Extreme Value Type I distributions are defined by their location and scale parameters only (i.e., they are two-parameter distributions and have no shape parameter). The PPCC's corresponding to these distributions were compared with the PPCC corresponding to the optimal shape parameter for the gamma distributional family.

The three-parameter gamma distribution is

$$f(z)=\frac{\left(\frac{z-\mu}{\beta}\right)^{\gamma-1} e^{-(z-\mu)/\beta}}{\beta\Gamma(\gamma)} \quad \text{for } z>\mu \tag{1}$$

(Johnson et al. 1994), where β, γ, and μ = scale, shape, and location parameter, respectively, and $\Gamma(\,)$ = gamma function.

The optimal distribution was determined for nine time-history records of wind-induced bending moments in low-rise buildings. The first eight records were generated from a low-rise steel building located in open terrain at 13 km inland near Miami. The building has a rectangular plan with dimensions $61\times30.5\ \text{m}^2$, a 6.1 m eave height, a gable roof with slope 1/24, and ridge parallel to the long building dimension. The wind-force resisting system consists of nine equally spaced two-hinged frames (Whalen et al. 1998). Aerodynamic pressures were measured at the University of Western Ontario at about 500 pressure taps installed on the envelope of a 1:200 wind tunnel model of the building (Lin and Surry 1997). The bending moment time histories at various cross sections and frames were computed for various wind directions using the software *WiLDE-LRS* (Whalen et al. 2000). The ninth record considered in the paper represents bending moments at the windward knee joint of a two-hinged center bay frame for a low-rise building whose model was tested in the Ruhr University Bochum wind tunnel (Kasperski et al. 1996).

Table 1 presents information on the nine records and results of the analyses, which show that the gamma distribution best fits all the nine records. A similar conclusion was reached by Gioffrè et al. (2000) for the ninth record on the basis of a visual comparison between the fits of the gamma and normal distributions.

The gamma distribution yields acceptable results only if the record's skewness coefficient is positive. If the skewness coefficient is negative, the gamma distribution can be used provided that the signs of the data are reversed. This was done for records 7 and 8. As was indicated earlier, in all nine cases the gamma distribution provides the best fit. Fig. 1 shows the PPCC plot for records 2 and 8 using the gamma distribution. Fig. 2 shows the probability plots for record 2 for the gamma distribution with optimal shape parameter, the normal distribution, and the Extreme Value Type I distribution. For details on the abscissa of the probability plots, see Filliben (1975) or Simiu and Scanlan (1996, p. 614).

Table 1. Summary of Statistical Analysis of Bending Moment Time Histories

Record	Wind[a] direction	Frame[b]	Section	Maximum (kN m)	Minimum (kN m)	Mean (kN m)	Standard deviation (kN m)	Skewness	Kurtosis	Normal distribution PPCC	Extreme Value 1 PPCC	Gamma distribution	
												Shape Parameter	PPCC
1	0	2	knee	640.9	−29.6	182.3	81.1	0.751	3.700	0.9839	0.9965	6.898	0.9997
2	20	2	knee	654.7	−11.9	209.7	83.7	0.644	3.713	0.9888	0.9947	9.857	0.9998
3	40	2	knee	656.6	−34.5	182.3	74.9	0.432	3.335	0.9947	0.9887	21.408	0.9998
4	70	3	knee	475.9	−90.5	123.2	55.1	0.548	3.638	0.9919	0.9924	13.776	0.9997
5	80	4	knee	511.9	−70.7	142.9	62.2	0.355	3.340	0.9964	0.9859	35.020	0.9997
6	90	5	knee	465.2	−31.7	155.8	66.7	0.437	2.993	0.9931	0.9878	18.286	0.9992
7[c]	0	2	ridge	19.3	−252.6	−74.0	32.2	−0.734	3.705	0.9848	0.9963	7.306	0.9998
8[c]	90	5	ridge	17.3	−142.4	−45.7	21.6	−0.343	2.850	0.9954	0.9842	29.122	0.9992
9		center	knee	115.3	13.1	53.1	15.0	0.566	3.314	0.9904	0.9924	11.939	0.9997

[a]Directions 0 and 90 signify wind parallel and normal to ridge, respectively.

[b]Frames 2 and 5 indicate next to the outer and center frame, respectively.

[c]For gamma distribution computations, the record is multiplied by −1 to make the skewness coefficient >0.

Because of their advantages in terms of computational efficiency, the maximum likelihood estimator (MLE) and the method of moments are preferable to the PPCC method for the purpose of routinely estimating the gamma distribution's shape parameter by the DAD software. For the nine records, Table 2 presents estimates of the shape parameter based on the MLE and the method of moments, and the corresponding PPCC estimates. Both estimators yield similar results, and the respective estimates of the correlation coefficients of the probability plots are very close to those obtained by the PPCC method. Fig. 3 shows that (using record 8 with the lowest PPCC value, see Table 2, after multiplication by −1 and using the moment estimators) the fit of the distribution to the data is quite acceptable. For implementation in the DAD software, the user is allowed to use either the MLE or the method of moments. The results shown in the remainder of this paper are based on the method of moments on account of its simplicity and faster execution.

Estimates are needed of both the maximum and minimum peak of each sample record. For convenience, in this paragraph reference is made only to the analysis of time series with positive skeweness. All statements applicable to such time series are also applicable to time series with originally negative skewness *after* their multiplication by −1. Each time series being considered then has a minimum (lower tail) peak and a maximum (upper tail) peak. While the gamma distribution is appropriate for representing the upper tail, it is not appropriate for representing the lower tail. Indeed, since the gamma distribution has a limited lower tail, the minimum peak would be limited to the location parameter μ, while in reality the minimum peak could be less than that value. Therefore, while the gamma distribution is appropriate for estimating the maximum peak, another distributional form needs to be sought for the estimation of the minimum peak. It was found that, for data smaller than the time series' sample mode, it is appropriate to assume the validity of a normal distribution. The sample mode is the estimator of the normal distribution's mean. The estimator for the standard deviation of the normal distribution is based on the data smaller than the mode. For record 6, the histogram, probability density function, cumulative frequencies, and cumulative distribution function are shown in Fig. 4, which shows that while the selected normal distribution does not fit well data larger than the mode—those data are fitted by a gamma distribution—it performs well for the data smaller than the mode. For the purpose of estimating the minimum peak, accuracy of the cumulative probability distribution is only required in the vicinity of the lower tail of the record.

To summarize, for time series with positive skewness, the gamma distribution with parameters determined by the MLE or the moment estimators is appropriate for estimating the maximum peak, while a normal distribution is appropriate for estimating the minimum peak. For records with negative skewness, the same conclusion holds after multiplication of the original time series by −1.

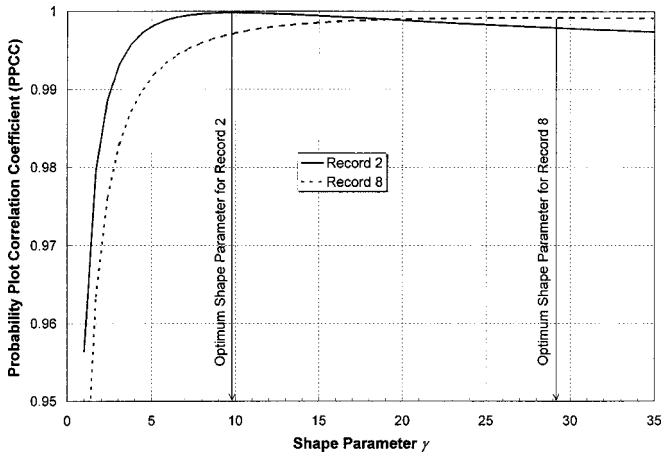

Fig. 1. Gamma distribution PPCC plots for records 2 and 8

Estimation of Peaks

Once the appropriate marginal probability distributions are obtained, the following procedure for estimating peak statistics, based on the translation processes approach, is followed. Consider a stationary non-Gaussian time series $x(t)$ with marginal distribution $F_X[x(t)]$ and duration T. This process is mapped onto a time series $y(t)$ with standardized marginal normal distribution $\Phi[y(t)]$. For the process $y(t)$, the cumulative distribution function of the largest peak $y_{pk,T}$ during time interval T is obtained by using classical results (Rice 1954)

$$F_{Y_{pk,T}}(y_{pk,T}) = \exp[-\nu_{0,y} T \exp(-y_{pk,T}^2/2)] \tag{2}$$

where $\nu_{0,y}$ = mean zero upcrossing rate of the Gaussian process $y(t)$. For a specified cumulative probability $F^i_{Y_{pk,T}}$, the above equation yields the corresponding maximum and minimum peaks

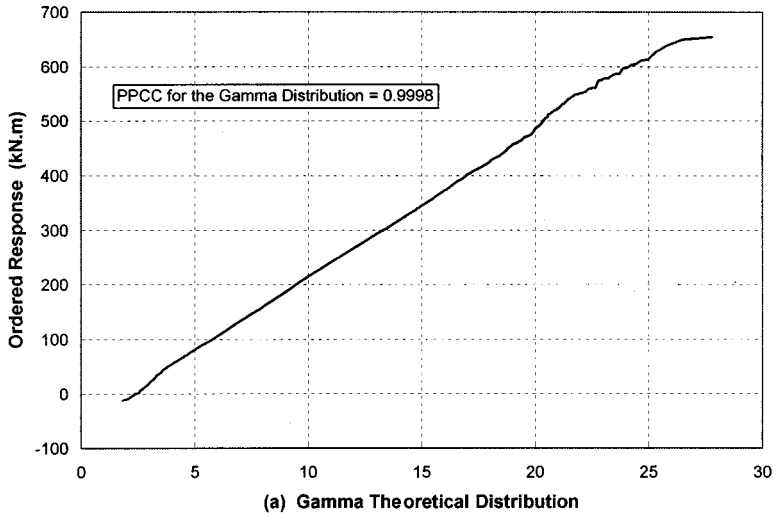

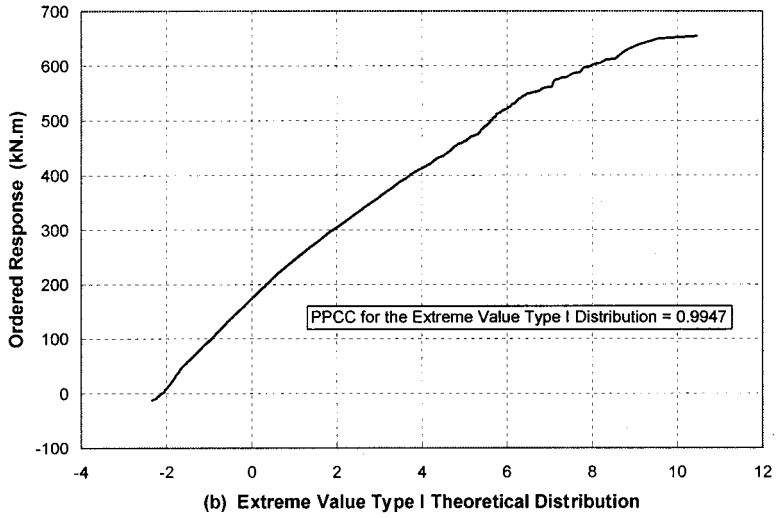

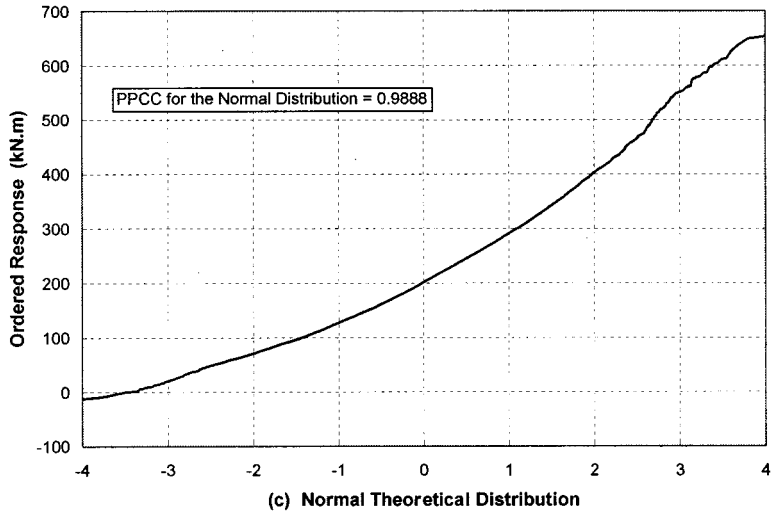

Fig. 2. (a) Gamma; (b) Extreme Value Type I; and (c) normal probability plots for record 2

Table 2. Probability Plot Correlation Coefficient using Maximum Liklihood Estimator and Moment Estimator for Gamma Distribution

	Maximum likelihood estimator		Moment estimator	
Record	Shape Parameter	PPCC	Shape Parameter	PPCC
1	7.729	0.9997	7.086	0.9997
2	10.494	0.9998	9.647	0.9998
3	21.531	0.9998	21.411	0.9998
4	13.998	0.9997	13.297	0.9997
5	36.048	0.9997	31.701	0.9997
6	12.313	0.9990	20.898	0.9992
7[a]	7.642	0.9998	7.428	0.9998
8[a]	19.260	0.9990	34.075	0.9992
9	10.971	0.9997	12.470	0.9997

[a]The record is multiplied by -1 to make the skewness coefficient >0.

$$y_{pk,T}^{\max,i}=\sqrt{2\ln\frac{-\nu_{0,y}T}{\ln F_{Y_{pk,T}}^{i}}} \quad \text{and} \quad y_{pk,T}^{\min,i}=-\sqrt{2\ln\frac{-\nu_{0,y}T}{\ln F_{Y_{pk,T}}^{i}}}$$

Two procedures for computing $\nu_{0,y}$ are considered. In the first procedure, x_u is defined as the height of the threshold of the process $x(t)$ that corresponds to a zero threshold in the process $y(t)$; i.e., at every time instant t for which $x(t)=x_u$, it is the case that $y(t)=0$. Thus, x_u is computed such that

$$\Phi[0]=F_X[x_u] \tag{3}$$

Since $\Phi[0]=1/2$

$$x_u=F_X^{-1}[1/2] \tag{4}$$

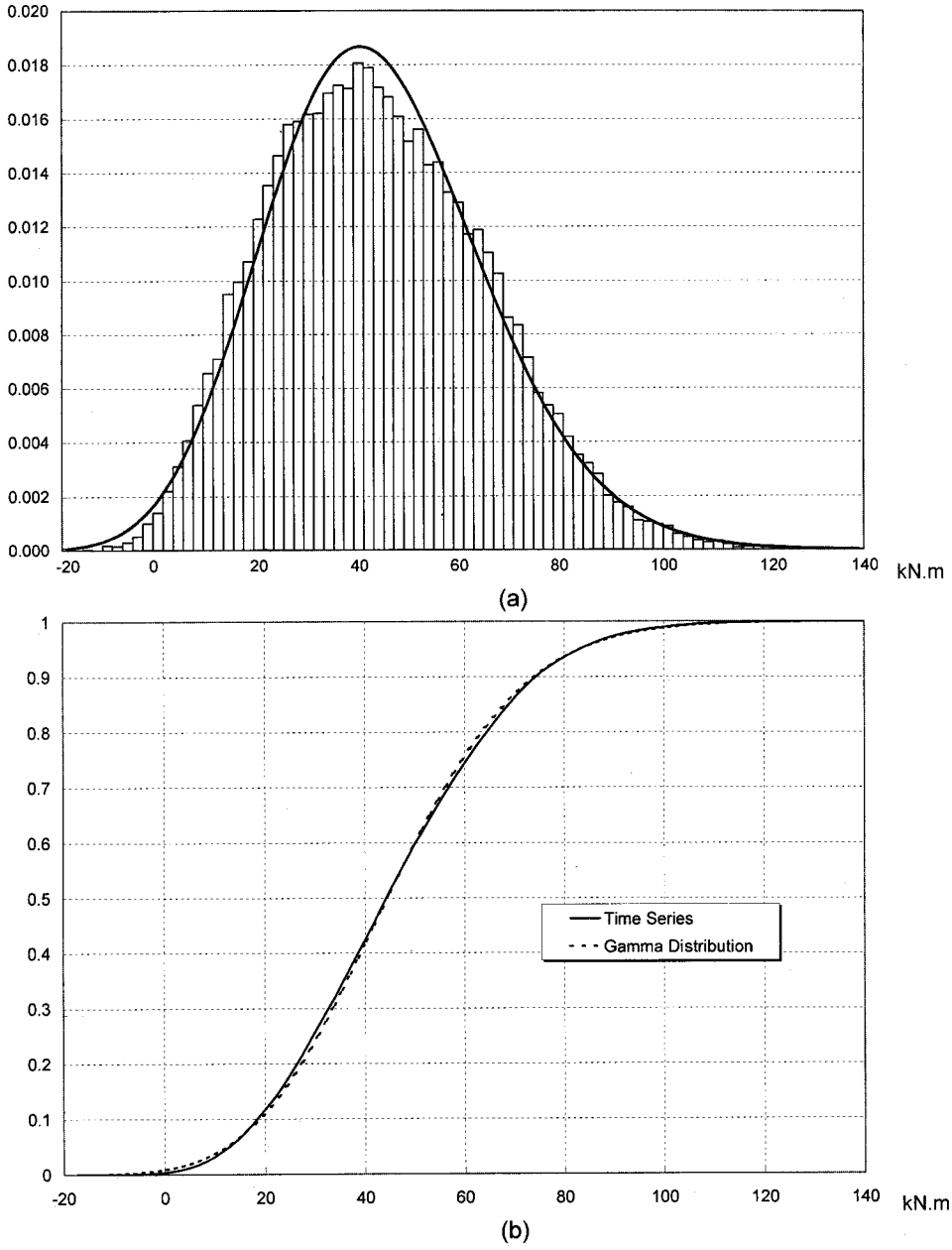

Fig. 3. (a) Data histogram and best-fitting gamma density function and (b) cumulative frequency and best-fitting gamma cumulative distribution function for record 8

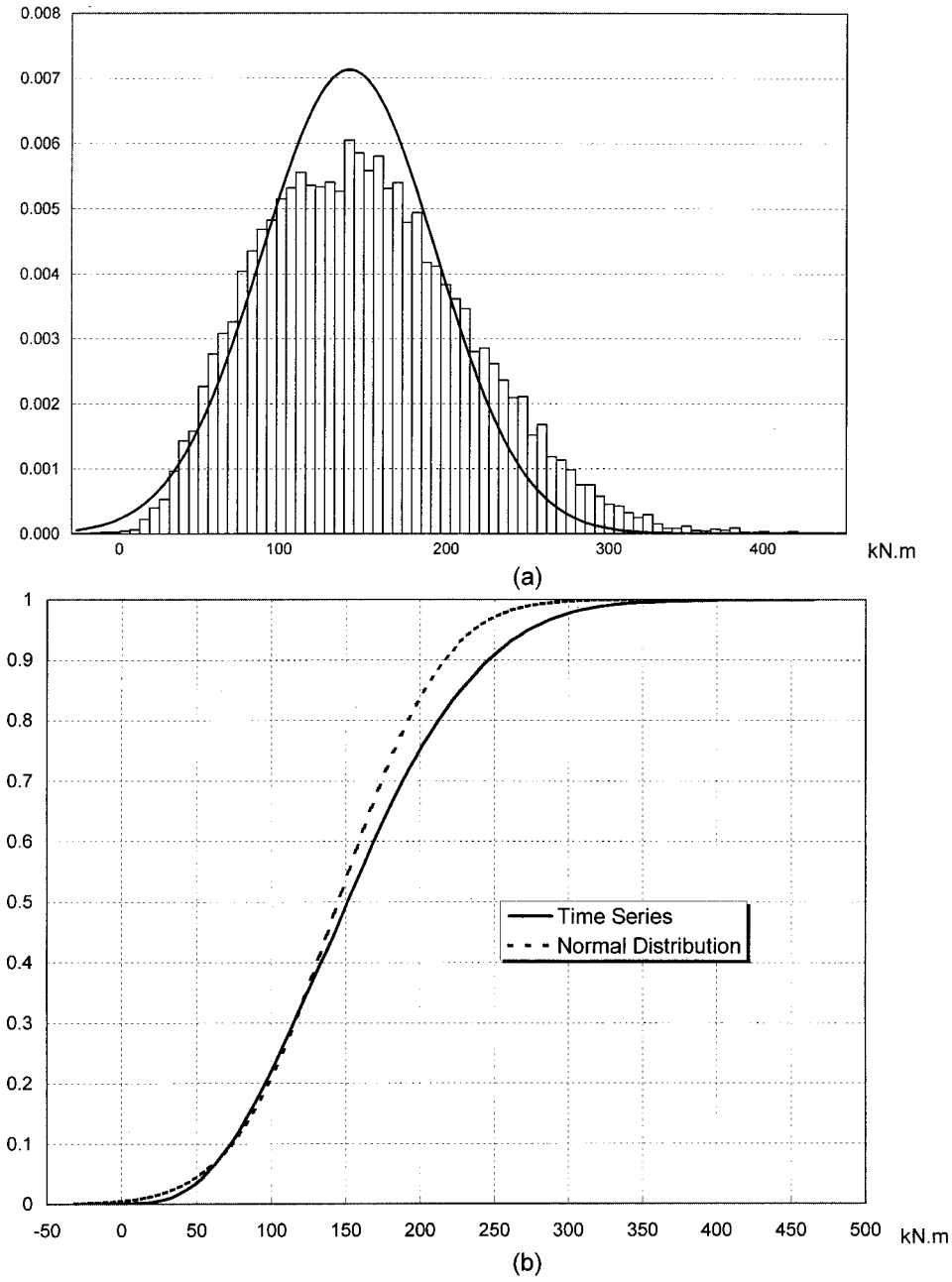

Fig. 4. (a) Data histogram and normal density function and (b) cumulative frequency and normal cumulative distribution function for record 6; normal distribution is fitted to lower end of histogram

Therefore, the mean zero upcrossing rate of the process $y(t)$, $\nu_{0,y}$, is equal to the mean upcrossing rate of the threshold x_u of the process $x(t)$, $\nu_{x_u,x}$

$$\nu_{0,y}=\nu_{x_u,x} \tag{5}$$

where $\nu_{x_u,x}$ is determined by counting the upcrossing rate of x_u of the process $x(t)$.

The second procedure for computing $\nu_{0,y}$ uses the classical result (Rice 1954)

$$\nu_{0,y}=\sqrt{\frac{\int_0^\infty n^2 S_y(n)dn}{\int_0^\infty S_y(n)dn}} \tag{6}$$

where n = frequency and $S_y(n)$ = spectral density function of process $y(t)$. In practice, it is assumed that $S_y(n)$ may be replaced by the spectral density function of process $x(t)$, $S_x(n)$. For spectral density shapes of the general type considered in this paper, the errors inherent in this assumption have been verified to be negligible (Grigoriu 1995).

It can be expected that the observed crossing rate is a less precise estimator of the true crossing rate $\nu_{0,y}$ than the estimator given by Eq. (6), which is based on the totality of the data contained in the sample. For this reason, Eq. (6) was chosen as an estimator of the zero upcrossing rates. It was found that Eq. (6) yields results that differ by as much as 40% from observed crossing rates. However, this has a minor effect on the estimated peaks, which were about 3% higher if Eq. (6) was used. Once the cumulative distribution function of the largest peaks, $F_{Y_{pk,T}}(y_{pk,T})$, is determined from Eq. (2), the distribution of the largest peaks of

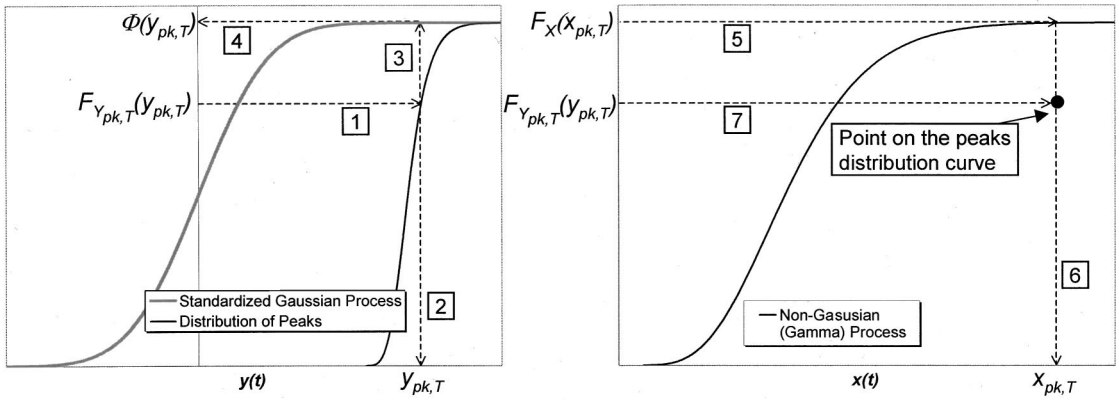

Fig. 5. Mapping procedure for a point from non-Gaussian process $x(t)$ to Gaussian process $y(t)$

$x(t)$ is estimated by mapping the peaks of the normally distributed time series on the non-Gaussian distribution space (Grigoriu 1995; Gioffrè et al. 2000). The procedure is illustrated in Fig. 5, where for a given cumulative probability of the peaks, $F_{Y_{pk,T}}(y_{pk,T})$, the Gaussian peak effect, $y_{pk,T}$, and its cumulative probability in the Gaussian space, $\Phi(y_{pk,T})$, are determined. The corresponding peak in the non-Gaussian space, $x_{pk,T}$, is then estimated corresponding to a cumulative probability of $F_X(x_{pk,T}) = \Phi(y_{pk,T})$.

Numerical Results

The procedure was applied to each of the nine time series being considered in this paper. For each time series with positive skewness, and for each time series obtained through multiplication of negatively skewed time series by -1, the output consists of the observed maximum and minimum peak, and the sample mean, sample standard deviation, 84, 97.5, and 99.9% of the maximum and minimum peak. These estimated 1 h peak statistics are presented in Table 3. For time series 1, Fig. 6 shows the best-fitting gamma distribution and the distributions of the maximum and minimum peaks.

An examination of the peak distribution for the nine records indicated that the distribution of the maxima and minima can be represented by the Extreme Value Type I (Gumbel) distribution. This is shown in Fig. 6 for record 1. Thus, the peak distribution can be determined once the mean and standard deviation of the peaks are estimated (see Simiu and Scanlan 1996; Johnson et al. 1994).

For Gaussian time series, the dispersion of the largest peak distribution is small, and the largest peak value commonly used in design is the mean value of the largest peak (Davenport 1964). For non-Gaussian time series, however, the dispersion of the peak is usually large and the observed peak may differ significantly from its mean value, as can be seen for the nine time series in Table 3.

This is not necessarily a matter for concern. Structural reliability estimates are based on what may be described, roughly, as a vectorial composition of the variability measures of the variates that produce the total wind effect. The variability of the total wind effect estimated as a result of such a composition is then used as a basis for estimating safety margins, including wind load factors (Ellingwood et al. 1980; Minciarelli et al. 2001). In any windstorm event, some of those variates can exceed the respective mean values. However, owing to the use of a safety margin for the total wind effect, this would not be significant from a structural safety point of view. Only if the dominant variates exceed the respective means by sufficiently large amounts will the structures exceed the limit state for which it was designed. The wind load factor is designed so that the probability of such exceedances is acceptably small.

The state of the art is ready for quantitative wind-related structural reliability calculations far more realistic and comprehensive

Table 3. Summary of Observed and Estimated, Maximum and Minimum Bending Moments

	Maximum peak (kN m)						Minimum peak (kN m)					
Record	Observed	Mean	Standard Deviation	84%	97.5%	99.9%	Observed	Mean	Standard Deviation	84%	97.5%	99.9%
1	640.9	640.4	55.0	691.7	771.8	900.3	−29.6	−41.2	15.0	−55.5	−76.1	−106.8
2	654.7	658.3	52.3	707.2	783.0	903.8	−11.9	−47.6	19.3	−66.0	−92.6	−132.0
3	656.6	545.7	39.0	582.3	638.0	725.6	−34.5	−61.0	17.9	−78.1	−102.8	−139.4
4	475.9	411.7	31.6	441.3	486.9	559.2	−90.5	−56.5	13.4	−69.3	−87.8	−115.4
5	511.9	436.1	29.9	464.3	506.9	573.3	−70.7	−75.1	17.2	−91.5	−115.2	−150.6
6	465.2	482.3	34.8	515.0	564.9	643.2	−31.7	−67.3	17.5	−83.9	−108.0	−143.7
7	19.3	17.7	6.4	23.8	32.7	45.9	−252.6	−255.1	21.5	−275.2	−663.2	−356.7
8	17.2	29.2	5.8	34.7	42.7	54.6	−142.4	−147.9	10.2	−157.6	−172.1	−194.8
9	115.3	126.4	8.9	134.9	147.8	168.1	13.1	7.8	3.8	4.2	−1.0	−8.6

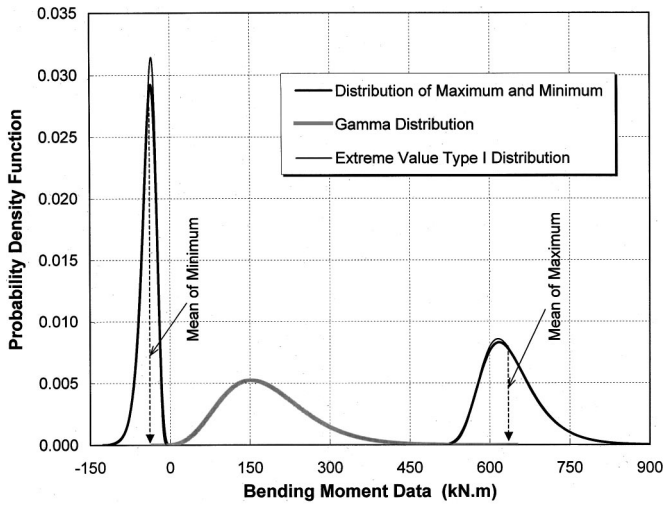

Fig. 6. Distribution of maximum and minimum peaks for record 1

than those that could be performed two decades ago (Minciarelli et al. 2001). However, until such calculations are performed in detail and evaluated by professional consensus, it is the writers' opinion that for structural design it is prudent to use peak values larger by some reasonable amount than their estimated means. It is suggested that this amount be, say, one standard deviation. In accordance with current practice, those peak effects would be converted into values for strength design through multiplication by the load factor specified in the ASCE 7 Standard. The use in this context of a peak equal to the mean peak plus one standard deviation is therefore judged to be conservative.

Influence of Record Duration and Sampling Rate

As mentioned earlier, the DAD software is used to perform large numbers of calculations. To reduce computation time, it may be helpful to input time series with less than 1 min wind tunnel duration, or with less than 400 Hz sampling rate (this rate is common for geometric model scales of about 1/200, say). The software module for estimating peaks developed in this paper can be used to investigate the effect of the record length and sampling rate on the estimated peaks.

In this study, various durations m hours were considered for that purpose, where $m=1.0$, 0.75, 0.67, 0.50, 0.33, and 0.25. The maximum and minimum 1 h peak statistics for records 1, 2, 4, and 5 are presented in Table 4. The statistics show the following: (1) for a prototype record duration of approximately 40 min ($m=0.67$), the estimated maximum peaks differ by about 3% or less from those of the corresponding 1 h record; the differences can be larger, however, for minimum peaks; (2) the estimated peaks—estimated as they are by using the entire information contained in the times series—are more stable than the observed peaks. This is clear from an inspection of records 2 and 4, in which the observed maximum peaks occur toward the 1 h records' ends, and differ significantly for 40 min and the 1 h record. In contrast, the respective peaks as estimated by the procedure described in the paper do not differ significantly.

As indicated earlier, for the first eight records of Table 1, the pressure time series were sampled in the wind tunnel at a rate $f=400$ Hz, which corresponds to a prototype rate of 7.28 Hz. In this study sampling rates f/n were considered, where $n=1$, 2, 3, 4, 5, and 6. For that purpose, two approaches were considered. In the first approach, for each sampling rate f/n, every nth point was selected from the original time series, thus a total of n cases

Table 4. Maximum and Minimum Bending Moment Statistics Considering Various Durations, m hours

		Maximum peak (kN m)						Minimum peak (kN m)					
Record	m	Observed	Mean	Standard Deviation	84%	97.5%	99.9%	Observed	Mean	Standard Deviation	84%	97.5%	99.9%
1	1.00	**640.9**	**640.4**	**55.0**	**691.7**	**771.8**	**900.3**	**−29.6**	**−41.2**	**15.0**	**−55.5**	**−76.1**	**−106.8**
	0.75	640.9	649.0	54.7	700.0	779.5	906.6	−29.6	−42.6	15.1	−57.0	−77.8	−108.7
	0.67	640.9	651.1	54.0	701.6	779.9	905.1	−29.6	−36.2	14.6	−50.1	−70.1	−100.0
	0.50	640.9	653.2	53.8	703.5	781.6	906.8	−29.6	−24.9	13.6	−37.9	−56.6	−84.4
	0.33	640.9	682.7	58.1	736.8	821.5	957.5	−29.6	−16.4	12.9	−28.6	−46.4	−72.7
	0.25	640.9	700.6	60.8	757.2	845.8	988.6	−7.4	−12.3	12.9	−24.5	−42.3	−68.6
2	1.00	**654.7**	**658.3**	**52.3**	**707.2**	**783.0**	**903.8**	**−11.9**	**−47.6**	**19.3**	**−66.0**	**−92.6**	**−132.0**
	0.75	612.5	637.2	47.5	681.7	750.1	858.1	−11.9	−51.9	19.7	−70.7	−97.9	−138.2
	0.67	612.5	643.5	48.3	688.8	758.3	868.4	−11.9	−57.2	20.2	−76.5	−104.2	−145.5
	0.50	612.5	619.4	44.7	661.4	725.5	826.4	−11.9	−61.2	20.5	−80.8	−108.9	−150.8
	0.33	597.5	610.8	43.8	652.1	714.7	813.0	−11.9	−69.4	20.9	−89.3	−118.0	−160.6
	0.25	529.8	574.7	38.5	611.1	665.6	750.2	−11.9	−92.8	23.8	−115.5	−148.2	−196.8
4	1.00	**475.9**	**411.7**	**31.6**	**441.3**	**486.9**	**559.2**	**−90.5**	**−56.5**	**13.4**	**−69.3**	**−87.8**	**115.4**
	0.75	475.9	414.6	31.9	444.5	490.6	563.8	−90.5	−54.9	13.3	−67.5	−85.9	−113.2
	0.67	475.9	420.0	32.3	450.2	496.7	570.6	−90.5	−54.8	13.3	−67.5	−85.9	−113.2
	0.50	403.3	397.0	28.5	423.8	464.7	528.9	−28.1	−62.7	14.5	−76.5	−96.4	−126.2
	0.33	403.3	400.9	28.1	427.3	467.4	530.3	−28.1	−81.2	17.5	−97.9	−121.9	−157.8
	0.25	341.8	388.1	26.1	412.8	449.9	507.8	−28.1	−91.4	18.9	−109.4	−135.4	−174.1
5	1.00	**511.9**	**436.1**	**29.9**	**464.3**	**506.9**	**573.3**	**−70.7**	**−75.1**	**17.2**	**−91.5**	**−115.2**	**−150.6**
	0.75	457.0	425.5	28.7	452.6	493.4	557.1	−70.7	−78.1	17.6	−94.9	−119.1	−155.3
	0.67	457.0	428.0	29.3	455.7	497.4	562.4	−70.7	−80.4	17.9	−97.4	−122.0	−158.6
	0.50	457.0	432.6	29.3	460.2	501.9	566.9	−39.0	−72.9	17.2	−89.3	−113.0	−148.2
	0.33	457.0	436.5	31.2	465.8	510.5	580.9	−39.0	−53.8	14.7	−67.9	−88.2	−118.4
	0.25	457.0	430.5	30.1	458.8	502.0	569.8	−35.9	−58.3	16.1	−73.6	−95.7	−128.6

Table 5. Maximum and Minimum Bending Moment Statistics Considering Various Sampling Rates, f/n

		Maximum peak (kN m)						Minimum peak (kN m)					
Record	n	Observed	Mean	Standard Deviation	84%	97.5%	99.9%	Observed	Mean	Standard Deviation	84%	97.5%	99.9%
1	1	**640.9**	**640.4**	**55.0**	**691.7**	**771.8**	**900.3**	**−29.6**	**−41.2**	**15.0**	**−55.5**	**−76.1**	**−106.8**
	2	618.3	621.4	54.8	672.5	752.2	879.8	−20.1	−32.8	13.9	−46.0	−65.0	−93.1
	3	625.1	610.8	54.6	661.8	741.0	867.7	5.1	−32.5	14.9	−46.7	−67.1	−97.3
	4	602.8	598.7	54.1	649.2	727.5	852.5	3.4	−27.6	14.3	−41.3	−60.8	−89.6
	5	576.8	588.0	53.6	638.1	715.5	838.9	5.2	−27.9	15.3	−42.6	−63.4	−94.2
	6	548.4	577.2	53.0	626.8	703.3	825.0	13.2	−22.5	14.1	−36.0	−55.1	−83.3
3	1	**656.6**	**545.7**	**39.0**	**582.3**	**638.0**	**725.6**	**−34.5**	**−61.0**	**17.9**	**−78.1**	**−102.8**	**−139.4**
	2	639.4	528.9	39.0	565.6	621.3	708.5	−29.5	−72.1	22.0	−93.1	−123.2	−167.8
	3	583.7	521.4	39.0	558.1	613.6	700.3	−29.7	−57.6	19.7	−76.4	−103.2	−142.9
	4	536.2	512.7	38.6	549.1	603.9	689.4	−29.0	−47.1	17.9	−64.1	−88.4	−124.3
	5	545.2	504.9	38.3	541.1	595.4	679.9	−27.6	−58.0	21.8	−78.9	−108.5	−152.1
	6	512.3	497.5	38.1	533.4	587.3	670.8	−28.9	−53.5	21.7	−74.2	−103.7	−146.9
6	1	**465.2**	**482.3**	**34.8**	**515.0**	**564.9**	**643.2**	**−31.7**	**−67.3**	**17.5**	**−83.9**	**−108.0**	**−143.7**
	2	451.9	465.6	34.9	498.4	548.2	626.2	−26.8	−68.4	19.2	−86.7	−113.0	−151.9
	3	452.6	457.3	34.7	489.9	539.3	616.4	−22.3	−51.9	16.8	−67.9	−90.8	−124.8
	4	421.1	448.8	34.5	481.3	530.2	606.5	−11.4	−59.1	19.3	−77.5	−103.8	−142.5
	5	415.8	441.3	34.3	473.7	522.3	597.9	−14.5	−74.6	23.4	−96.9	−128.7	−175.4
	6	408.5	434.3	34.2	466.6	514.9	589.8	−10.7	−62.2	21.9	−83.1	−112.6	−156.1
7	1	**19.3**	**17.7**	**6.4**	**23.8**	**32.7**	**45.9**	**−252.6**	**−255.1**	**21.5**	**−275.2**	**−663.2**	**−356.7**
	2	12.8	14.2	6.0	19.9	28.2	40.4	−241.5	−248.0	21.4	−267.9	−299.1	−348.9
	3	8.4	12.8	6.1	18.7	27.0	39.3	−230.4	−243.4	21.3	−263.2	−294.1	−343.4
	4	7.7	11.4	6.1	17.3	25.6	38.0	−228.5	−238.1	21.0	−257.7	−288.2	−336.7
	5	−3.1	9.6	6.0	15.4	23.6	35.7	−230.4	−233.7	20.8	−253.1	−283.2	−331.2
	6	−3.6	9.0	6.3	15.0	23.5	36.0	−217.9	−229.2	20.6	−248.5	−278.2	−325.5

corresponding to different starting time instants may be used. In the second approach, the time series were resampled at a lower rate f/n after low-pass filtering the original time series using a Chebyshev type I low-pass filter with a cutoff frequency of $0.4f/n$. The latter approach is already implemented in *MATLAB* (Math Works 2000). The two approaches yielded similar results. The maximum and minimum 1 h peak statistics for records 1, 3, 6, and 7 using the second approach are presented in Table 5. The results show the following: (1) for $n=2$ (200 Hz sampling rate) the effect of the sampling rate reduction on the estimated peaks is acceptable, especially for the larger peak; (2) estimated peaks are more stable than observed peaks. This can be seen by comparing the results from the original frequency ($n=1$) to those with larger n's. While reductions in sampling frequency can significantly affect the observed peaks, their effect on estimated peaks tends to be less severe.

The extent to which the record length or the sampling rate may be reduced needs to be tested numerically for each type of structure. Reduced record lengths and reduced sampling rates can be used in calculations only if results of the numerical tests show that the effects on the estimation of the peaks are acceptable.

Conclusions

In this paper, an automated procedure was developed for estimating peaks of non-Gaussian processes representing wind-induced internal forces in frames of low-rise buildings. The procedure was designed to complement software for the database-assisted design (DAD) of low-rise building frames. As a first step in the development of the procedure, statistical tests were performed which indicate that, for the purpose of estimating peaks, the gamma distribution and the normal distribution are appropriate models for the marginal distribution fitting of the longer and the shorter tail of internal force histograms, respectively. The input to the procedure consists of time series of the internal forces calculated by using the DAD approach. The output consists of sample means, standard deviation, and quantiles of the respective time-series peaks. It was found that the distribution of the peaks can be represented by the Extreme Value Type I (Gumbel) distribution.

The procedure was used to investigate the influence of the time-series duration and sampling frequency on the estimated peaks. It was found that the peaks estimated by the proposed procedure are less dependent than observed peaks on record length and sampling rates. Reductions of record lengths and sampling rates can result in substantially smaller data storage requirements and computation times. However, the software developed in this paper should be used to verify for typical records of the structure of interest that the effects of such reductions on the estimation of peaks are acceptably small.

Acknowledgments

The writers acknowledge with thanks the assistance of N. A. Heckert of the Statistical Engineering Division, National Institute of Standards and Technology, with the *Dataplot* software. Exchanges with M. Grigoriu of Cornell University on the characteristics of non-Gaussian processes are also acknowledged with thanks. Certain trade names or company products are mentioned in the text to specify adequately the procedure used. In no case does such identification imply recommendation or endorsement by NIST, nor does it imply that the product is the best available for the purpose.

References

ASCE Standard 7-98 (1998). *Minimum design loads for buildings and other structures*, Structural Engineering Institute, American Society of Civil Engineers, Reston, Va.

Dataplot. (1996). ⟨http://www.itl.nist.gov/div898/software/dataplot/document.htm⟩.

Davenport, A. G. (1964). ''Note on the distribution of the largest value of a random function with application to gust loading.'' *J. Inst. Civ. Eng.*, 24, 187–196.

Ellingwood, B. R., Galambos, T., McGregor, J., and Cornell C. A. (1980). *Development of a probability based load criterion for American National Standards A58*, NBS Special Publication 577, National Bureau of Standards, Washington, D.C.

Filliben, J. J. (1975). ''The probability plot correlation coefficient test for normality.'' *Technometrics*, 111–117.

Gioffrè, M., Grigoriu, M., Kasperski, M., and Simiu, E. (2000). ''Wind-induced peak bending moments in low-rise building frames.'' *J. Eng. Mech.*, 126(8), 879–881.

Grigoriu, M. (1995). *Applied non-Gaussian processes*, Prentice Hall, Englewood Cliffs, N.J.

Johnson, N. L., Kotz, S., and Balakrishnan, N. (1994). *Continuous Univariate Distributions, Volumes I and II*, 2nd Ed., Wiley, New York.

Kasperski, M., Koss, H., and Sahlmen, J. (1996). ''BEATRICE joint project: Wind action on low-rise buildings. Part I. Basic information and first results.'' *J. Wind. Eng. Ind. Aerodyn.*, 64, 101–125.

Lin, J., and Surry, D. (1997). *Simultaneous time series of pressures on the envelope of two large low-rise buildings*, BLWT-SS7-1997, Boundary Layer Wind Tunnel Laboratory, Univ. of Western Ontario, London, Ontario, Canada.

Math Works, Inc. (2000). *Matlab Reference Manual Version 6*, Math Works, Inc., Natick, Mass.

Minciarelli, F., Gioffrè, M., Grigoriu, M., and Simiu, E. (2001). ''Estimates of extreme wind effects and wind load factors: Influence of knowledge uncertainties.'' *Probalistic Eng. Mech*. 16, 331–340.

Rice, S. O. (1954). ''Mathematical analysis of random noise.'' *Select papers on noise and stochastic processes*, N. Wax, ed., Dover, New York.

Simiu, E., and Scanlan, R. H. (1996). *Wind effects on structures*, 3rd Ed., Wiley, New York.

Whalen, T., Simiu, E., Harris, G., Lin, L., and Surry, D. (1998). ''The use of aerodynamic databases for the effective estimation of wind effects in main wind-force resisting systems: Application to low buildings.'' *J. Wind. Eng. Ind. Aerodyn.*, 77–78, 685–693.

Whalen, T., Shah, V., and Yang, J. S. (2000). *A pilot project for computer-based design of low-rise buildings for wind loads—The WiLDE-LRS user's manual, NIST GCR 00-802*, National Institute of Standards and Technology, Gaithersburg, Md.